AUT Journal of Electrical Engineering

AUT J. Elec. Eng., 49(2)(2017)131-140
DOI: 10.22060/eej.2017.12155.5050

Performance Analysis Of Mono-bit Digital Instantaneous Frequency Measurement (Difm) Device

Y. Norouzi[1*], H. Shahbazi[2], S. Mirzaei[3]

[1] Dept. of Elrctrical Engineering, Amirkabir University of Technology, Tehran, Iran

[2] Dept. of Science and Research, Azad University, Tehran, Iran.

[3] School of Engineering Science, College of Engineering, University of Tehran,Tehran, Iran

ABSTRACT: Instantaneous Frequency Measurement (IFM) devices are the essential parts of any ESM, ELINT, and RWR receiver. Analog IFMs have been used for several decades. However, these devices are bulky, complex and expensive. Nowadays, there is a great interest in developing a wide band, high dynamic range, and accurate Digital IFMs. One Digital IFM that has suitably reached all these requirements is mono-bit zero-crossing IFM, made by some different producers at present. In this paper, the performance of mono-bit digital Instantaneous Frequency Measurement (IFM) device is analyzed. This analysis includes quantization error, thermal noise, clock jitter, comparator bias and also "Pulse-on-Pulse" occurrence. The error limits due to all these factors are computed and analyzed, and a unified approach to the system design is presented.

Review History:

Received: 12 November 2016
Revised: 30 August 2017
Accepted: 3 September 2017
Available Online: 15 October 2017

Keywords:
Digital Instantaneous Frequency Measurement (DIFM)
Mono-bit Receiver
Zero-crossing

1- Introduction

Instantaneous Frequency Measurement (IFM) unit is an essential part in any ESM device. Nowadays, even very simple Radar Warning Receivers (RWR) includes an IFM. The wideband instantaneous frequency measurement (IFM) receiver offers a high probability of intercept over wide instantaneous RF bandwidth, high dynamic range, good sensitivity and high-frequency measurement accuracy [1].

The development of analog IFM receivers dates back to several decades ago. The analog IFM is basically a crystal video receiver along with a frequency sensing method. A usual frequency sensing method divides the signal into two paths with a short delay inserted in one path. If the amount of delay is equal to T, then the phase difference between the two signals will be equal to $\Delta\phi=2\pi fT$. Thus, if the phase difference between these two signals is compared via a phase comparator, the result will be proportional to the signal frequency (see Figure 1).

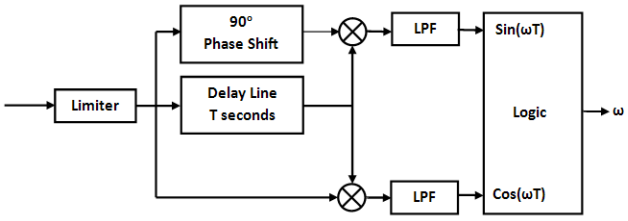

Fig. 1. Basic block diagram of an IFM receiver

It is known that the phase is only unambiguous within 2π radians. It means that with a fixed delay line of T seconds, the unambiguous frequency range of IFM is equal to 1/T. Naturally, the output of the IFM discriminator is also proportional to the signal amplitude. Hence, in order to eliminate this undesirable effect, a limiting amplifier should precede the discriminator. In such a system, noise limited sensitivity is achieved. However, a separate crystal video amplitude channel is required to operate as a threshold detector, which determines the times at which there is sufficient signal level to consider the discriminator output valid. With a limiter, an accurate frequency measurement over a dynamic range of 70 dB or more is practical [2]. However, as any other receiver, including a limiting amplifier, this incorporates capture effect, which means that whenever the IFM input consists of more than one signal, the system only responds to the strongest one and the other signals would not have any considerable effect on the output of the system [3]. Accordingly, the main drawback of a conventional IFM receiver is its incapability to handle "Pulse-on-Pulse" situations.

Weiss and Friedlander in [4] analyzed this problem in IFM receivers. In [5], the situation in which "Pulse-on-Pulse" occurrence can produce an error in frequency measurement of even the stronger signal was analyzed

In [6], Hedge et al. proposed an IFM system with two correlators in order to handle "Pulse-on-Pulse" situation. Gruchalla and Czyzewski analyzed the performance of IFM receiver in a dense electromagnetic environment [7]. In the paper [8], the same authors in collaboration with Slowik suggested some solutions to resolve the "Pulse-on-Pulse" problem in common analog IFM receivers.

Also, some other authors tried to improve the other aspects of generic IFM scheme. For example, in [9] Thornton proposed some solutions to extend the bandwidth of IFM receivers. Furthermore, Chandra et al. in [10] worked on the zero-crossing points of the signal to find an optimal estimation of the frequency of the signal.

The corresponding author; Email: y_norouzi@aut.ac.ir

In order to achieve an accurate estimate of frequency, analog IFM receivers need several delay lines (usually four or five) and the lengthiest of them should have a delay of the tenth or even hundreds of nano-seconds. This fact makes IFM receiver bulky, especially when it is designed to work on higher microwave frequency bands in which low loss waveguides should be used to produce the delay line. In addition, the temperature of these delay lines should be maintained constant in order to have a constant delay time. This fact necessitates an oven for the IFM receiver. All of the above-mentioned facts make the generic IFM receivers unattractive if some alternative solutions exist. This fact is emboldened if we consider that despite all solutions suggested for "Pulse-on-Pulse" problem, the performance of analog IFM receiver is not usually acceptable.

The problems incorporated in analog IFMs have attracted some authors to search for other schemes for the wide band frequency measurement. For example in [11] and [12] Xihua et al. developed some frequency measurement schemes based on optical methods. However, the most attractive alternative solution for analog IFMs is their digital counterpart. The basic idea of digital IFM is simply sampling the signal with a high sampling rate and, then, taking the fast Fourier transform (FFT) of the signal. However, this basic solution is not very attractive because it requires a sampling rate in the order of several giga-samples per second for a wide-band operation. These high sampling rates in combination with sufficient resolution bits providing reasonable dynamic range have not been achieved yet. Moreover, calculating the FFT of the signal which is sampled at such a high sampling rate needs a tremendous logic, making the system bulky, complex and expensive. Despite all these problems, some authors have proposed a simplified version of this generic digital IFM with a limited bandwidth. In [13], Helton et al. developed such an idea to construct a digital IFM with 1.2GHz bandwidth. In [14], Tsui presented 1 and 2 bit FFT method to eliminate the need to high complex computation for digital IFM. However, he showed that the instantaneous dynamic range of such a system is limited to only 5dB. Some other authors presented a mixed combination of digital and analog IFMs to achieve the benefits of the both of them (i.e. digital and analog method) [15].

However, the most attractive applied digital method for frequency measurement is the zero-crossing scheme which is currently used by ELISRA corporation [16] and INPHI-TECH [17] in their IFM products. In this method, the signal is sampled using a single bit. It means that only the signal of signals are samples. These samples are then used to count the number of zero-crossing points in a pre-determined time interval (e.g. 100ns). Now, if the signal contains only one sinusoid, then the number of zero-crossing points has enough information to estimate the frequency of the signal with sufficient accuracy.

Some recent works on IFM are as follows. In [18] Ivanov et al. used frequency-to-amplitude conversion in fiber optics as a method for Instantaneous Frequency Measurement. In [19] the authors used Bragg grating structure to implement IFM on a silicon chip. In [20], a multi-band stop filter structure is used for IFM.

In this paper, the zero-crossing method is discussed. In Section 2, the basic scheme is described and analyzed in order to find the cause of frequency measurement errors. Based on these calculations, in Section 3, it is described how a little change to this basic scheme can improve the frequency measurement accuracy considerably. Section 4 illustrates how the "Pulse-on-Pulse" occurrence can be detected and how in some special cases the frequency of both signals can be estimated. In sections 5, 6 and 7, the effects of thermal noise, clock jitter, and comparator bias on the performance of the system are analyzed. In section 8, it is demonstrated that how the above-mentioned effects can restrict the suitable frequency coverage range of the system. In section 9, all the considerations of previous sections are reviewed, a general and unified algorithm for the system is provided, and the results of different derived approximate equations are compared with simulations. Finally, the conclusion part of this paper is presented in section 10.

2- The proposed method

As mentioned earlier, in a mono-bit digital IFM, a signal is sampled at a rate equal to f_s and any sample, say $x(kT_s)$, is converted to a bit, a_k, according to the following eqaution:

$$a_k = \begin{cases} 0 & \text{if} \quad x(kT_s) < 0 \\ 1 & \text{otherwise} \end{cases} \tag{1}$$

Then, the number of zero-crossings is calculated using the following logical operation:

$$z = \sum_{k=1}^{N} a_k \oplus a_{k-1} \tag{2}$$

Here $\oplus$ stands for logical XOR and a_ks are digitized samples of a signal which are produced using the following comparison:

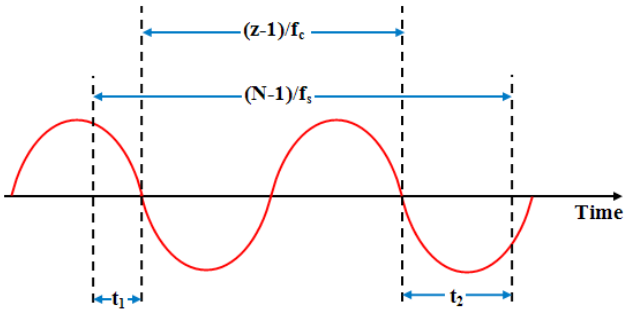

Fig. 2. Relationship between number of zero-crossings and frequency of signal

According to Figure 2, we have:

$$\frac{z-1}{2f_c} + \Delta t = \frac{N-1}{f_s} \quad (\Delta t = t_1 + t_2) \tag{3}$$

According to Figure 2, z is the number of zero-crossings of the analog signal and N denotes the number of digital samples of the signal. Actually, if the first and the last samples coincide with the first and the last zero-crossing, then the frequency estimate is out of error, but it does not usually happen. In this equation, both t_1 and t_2 have a uniform distribution between 0 and $0.5f_c$, thus Δt has a triangular distribution between 0 and $1/f_c$. This equation can be rewritten as:

$$f_c = \frac{z-1}{2(N-1)-2\Delta t f_s} f_s = \frac{(z-1)f_s}{2} \times \frac{1}{N-1-u f_s / f_c} \tag{4}$$

Here, u is a random variable, with a distribution similar to Δt,

but scaled by f_c. Solving this equation for f_c, we have:

$$f_c = \left(\frac{z-1}{2} + u\right)\frac{f_s}{N-1} \tag{5}$$

The mean of the random variable u is equal to 0.5 and its standard deviation is 0.32; hence, the LMSE estimate of f_c and the rms error associated with this estimation are equal to:

$$\hat{f_c} = \frac{z f_s}{2(N-1)}, \qquad \Delta f_{rms} = \sqrt{\frac{5}{48}}\frac{f_s}{N-1} \cong \frac{0.32 f_s}{N-1}. \tag{6}$$

2- 1- Modification of the basic method

As was mentioned in the previous section, the main cause of error in frequency estimation is Δt, i.e. the actual zero-crossing points and the location of the first and the last digital sample. In order to reduce the effect of this error, it is possible to count all samples before the first and after the zero-crossing points. Doing so, there remain N_1 samples and we have:

$$\frac{z-1}{2f_c} + \Delta\hat{t} = \frac{N_1 - 1}{f_s} \quad ,(\Delta\hat{t} = \hat{t}_1 + \hat{t}_2) \tag{7}$$

Here, t_1 is the time difference between the first digital and first zero crossing. Also, t_2 is the difference between the last zero-crossing and the last digital sample and N_1 is the number of samples in between (refer to Figure 2). Here, $\hat{t}_1$ and $\hat{t}_2$ are uniformly distributed between 0 and $1/f_s$, and are independent of f_c. Thus, we have:

$$f_c = \frac{(z-1)f_s}{2}\frac{1}{(N_1-1) - f_s\Delta\hat{t}} \tag{8}$$

In this equation $f_s\Delta\hat{t}$ is between 0 and 2. Therefore, it is many times smaller than (N_1-1). This fact can help us to approximate the above equation as:

$$f_c \cong \frac{(z-1)f_s}{2(N_1-1)}\left(1 + \frac{f_s}{N_1-1}\Delta\hat{t}\right) \tag{9}$$

This linear equation can be used to find the LMSE estimate of f_c and the rms error of this estimation by:

$$\hat{f_c} \cong \frac{N_1(z-1)f_s}{2(N_1-1)^2}, \qquad \Delta f_{rms} = \frac{(z-1)f_s}{2(N_1-1)^2}\sqrt{\frac{5}{48}} = \frac{0.32 f_c}{N_1}. \tag{10}$$

Always f_c is less than half of f_s; thus, the rms error of the modified method is at most half that of the basic method. However, for smaller f_c values, the difference between the accuracy of these two methods is significant. Furthermore, in the proposed method, there is no need to repeat the calculation with half, one quadrant and … of the original sampling rate in order to obtain a higher accuracy.

In Figure 3, equation (10) is compared with simulation results. As shown, the mean value of the quantization error is the same as that of (10). However, the exact error is a function of input frequency. Actually, for input frequencies equal to $f_s/2^n$, the error is minor, while for some other frequencies, the error may be about 1.7 of that given by (10).

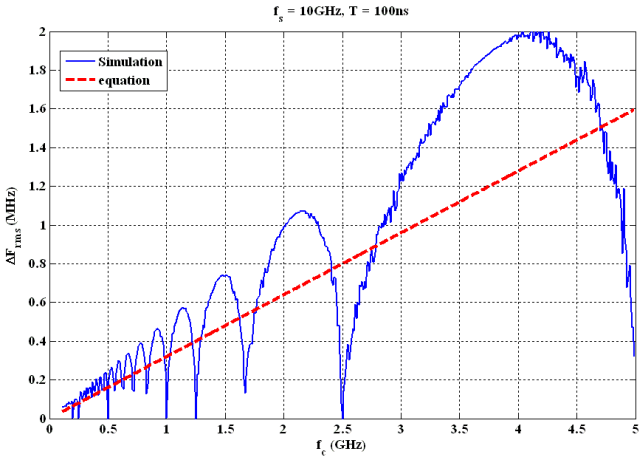

Fig. 3. Quantization error (a comparison between equation 10 and simulation result)

2- 2- Pulse on pulse detection

As mentioned earlier, one of the main drawbacks of analog IFM receivers is their incapability to handle "Pulse-on-Pulse" situation. In a busy electromagnetic spectrum or when a continuous wave (CW) source exists, this inability can cause a great difficulty. Therefore, in any IFM scheme, the performance against "Pulse-on-Pulse" situation should be analyzed carefully.

The method proposed in the previous sections is based on the zero-crossings of the signal. If the signal contains only a pure sinusoid, then all its zero-crossings should be separated by $1/2f_c$. As mentioned in [21], usually a uniform zero-crossing represents a pure sinusoid. There are very rare cases in which a combination of more than a single sinusoidal signal can produce a uniform zero-crossing pattern. Thus, any deviation from a uniform zero-crossing may represent a "Pulse-on-Pulse" situation. However, as it will be explained in the next section, the existence of thermal noise can divide the distance between two consequent zero-crossing points to two sections, hence producing a non-uniform pattern. However, again as it will be explained later in the next section, such an occurrence is probably only once within the sampling window. Regarding this fact, the following algorithm can help us determine a "Pulse-on-Pulse" occurrence:

1- count the samples between all consequent zero-crossing points (k_is).
2- delete the two smallest values of k_is.
3- in remaining k_is, determine the difference between the smallest and the greatest one (d).
4- if d is higher than two samples, then a "Pulse-on-Pulse" situation occurs; otherwise, the pulse is a pure sinusoid.

The above-mentioned algorithm can determine whether a "Pulse-on-Pulse" has occurred or not; this can help us to solve the problem to some extent. But usually, we want to determine the frequency of both sinusoids existing in the pulse. Assume that we have the following signal:

$$x(t) = A_1\sin(\omega_1 t) + A_2\sin(\omega_2 t + \phi) \tag{11}$$

Without any further assumption, it is not easy to determine the zero-crossing behavior of this signal in an understandable manner. Thus, we assume that A_2 is much smaller than A_1. At the end of this section, we will refer again to this assumption to analyze its validity requirements. We assume that $A_2 \ll A_1$. If A_2 is equal to zero, then the number of zero-crossing points of the signal are equal to $t_k=k/2f_1$. With a non zero A_2 , the zero-crossings change by a little amount equal to Δtk. Thus we have:

$$0 = A_1 \sin\left(\omega_1\left(t_k+\Delta t_k\right)\right)+A_2 \sin\left(\omega_2\left(t_k+\Delta t_k\right)+\phi\right)\cong$$
$$A_1\left(\sin\left(\omega_1 t_k\right)+\omega_1\Delta t_k \cos\left(\omega_1 t_k\right)\right)+A_2 \sin\left(\omega_2 t_k+\phi\right)= \quad (12)$$
$$-A_1\omega_1\Delta t_k\left(-1\right)^k+A_2 \sin\left(\frac{\pi k f_2}{f_1}+\phi\right)$$

Therefore we have:

$$\Delta t_k \cong \frac{A_2\left(-1\right)^k}{A_1\omega_1}\sin\left(\frac{\pi k f_2}{f_1}+\phi\right) \quad (13)$$

Hence the zero-crossing is modulated with a sinusoid with a carrier frequency of f_2. This signal is sampled at a rate equal to $2f_1$. Thus, if f_2 is less than f_1 and also f_1 less than $\frac{A_2}{2\pi A_1}f_s$ (this is the necessary condition for changing the zero crossing at least by one sample) , then f_2 can be calculated using different frequency estimation methods, e.g. the method explained in [22] and [23]. Otherwise, the existence of the second sinusoid cannot be detected or its true frequency cannot be estimated correctly.

In the beginning of this section, we assumed that the amplitude of the second sinusoid is much less than the first one. Now, we are to analyze the validity using the results of Figure 4. In this simulation, a pulse with 100ns length contains two sinusoids. The first one is a 1GHz signal with unit amplitude, the second has a frequency equal to 400MHz, and an amplitude less than or equal to the first one. This signal is sampled at a rate equal to 10GHz. The zero crossings are calculated using equation (2). Then, the changes in zero-crossing points around the mean value are derived and the FFT of this signal is calculated. The result is represented in Figure 4. It can be shown that, while f_2 is less than f_1, even with the same amplitudes it is possible to find the frequency of the second pulse with an acceptable accuracy. The result is valid at least within a 40dB dynamic range. However, when f_2 is greater than f_1, then the spectrum folds over f_1 and the true f_2 value becomes ambiguous. Although not represented in these figures, when f_1 or f_2 increases and approaches $f_s/2$, the result will not become highly satisfying.

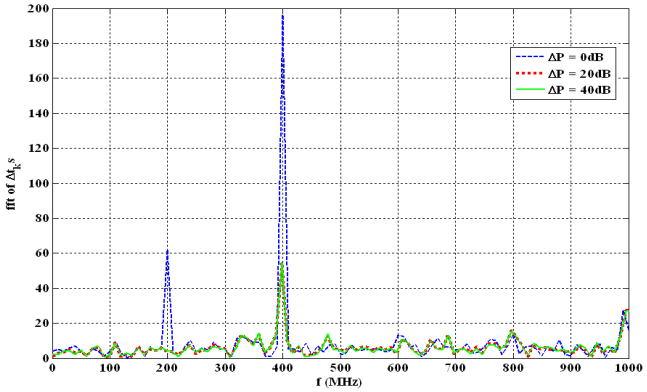

Fig. 4. Effect of pulse on pulse situation on variation in zero-crossing points (f_s = 10GHz, f_1 = 1GHz, f_2 = 400MHz)

3- Effect of imperfections

3- 1- Effect of additive noise

The various effects of a thermal noise on the frequency measurement process are presented in Figure 5.

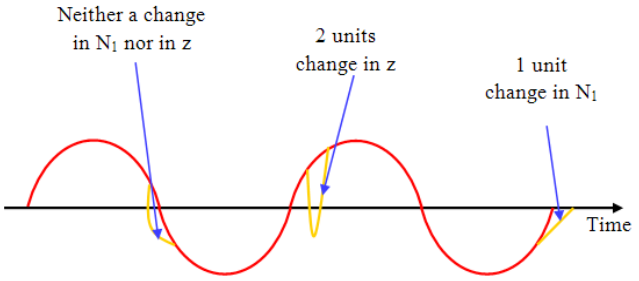

Fig. 5. Various effects of a thermal noise on frequency measurement algorithm

With referring to Figure 5, one can say that the additive noise may be effective only when it is so strong such that it can change the sign of a sample. In this case, even if the sign changing the sample be next to a zero-crossing point within the sampling window, the noise has no effect on the estimated frequency. The only result of such an event can be a "Pulse-on-Pulse" declaration. If the sign changing the sample is inside the sampling window but not near any zero-crossing point, then it adds 2 units to z. As a result, the estimated f_c changes by

$$\Delta f_1 = \frac{N_1 f_s}{\left(N_1-1\right)^2} \cong \frac{f_s}{N_1} \quad (14)$$

The probability of such an event is calculated by

$$P_1 = \frac{4}{2\pi}\int_{2\pi f_c T_s}^{\pi/4} Q\left(\frac{A\sin\theta}{\sigma_N}\right)d\theta \quad (15)$$

Here, A is the amplitude of the input sinusoidal signal and σ_N is the standard deviation of the noise. The above equation can be solved only numerically. Our numerical analysis shows that the above equation can be approximated by the following one:

$$P_1 \cong \frac{Q\left(\frac{A}{\sigma_N}\sin\left(2\pi\frac{f_c}{f_s}\right)\right)^{1.136}}{7.877} \quad (16)$$

The above relation is easier to handle than the relation (15). On the other hand, if the additive noise changes the sign of the first or the last sample, then it can increase or decrease N1 by 1, resulting in the following frequency estimation error:

$$\Delta f_2 \cong -\frac{(z-1)N_1 f_s}{2(N_1-1)2N_1} = -\frac{f_c}{N_1} \quad (17)$$

The probability of such an error is calculated by:

$$P_2 = \frac{4}{2\pi}\int_0^{2\pi f_c T_s} Q\left(\frac{A\sin\theta}{\sigma_N}\right)d\theta \quad (18)$$

Again, it can be numerically shown that (18) can be suitably approximated by the following one,

$$P_2 \cong \frac{0.899^{SNR(dB)}}{3.93} = 0.25\left(\frac{\sigma_N}{A}\right)^{0.92} \quad (19)$$

Now the mean and rms error in frequency measurement due to additive noise are obtained from

$$\mu_f = P_1 \times \Delta f_1 + 2P_2 \times \Delta f_2$$
$$\Delta f_{rms} = \sqrt{P_1 \times (\Delta f_1)^2 + 2P_2 \times (\Delta f_2)^2} \quad (20)$$

Here, it is assumed that P_1 is small enough so that only one change in the sign is probably within the sampling window. Using the above-mentioned inequalities, we have:

$$\Delta f_{rms} \cong \sqrt{(z-1)\frac{Q\left(\frac{A}{\sigma_N}\sin\left(2\pi\frac{f_c}{f_s}\right)\right)}{7.877}\times\left(\frac{f_s}{N_1}\right)^2 + \frac{\left(\frac{\sigma_N}{A}\right)^{0.92}}{1.96}\times\left(-\frac{f_c}{N_1}\right)^2}$$
$$= \frac{f_s}{N_1}\sqrt{0.25N_1\beta Q\left(\frac{A}{\sigma_N}\sin(2\pi\beta)\right) + 0.51\left(\frac{\sigma_N}{A}\right)^{0.92}\times\beta^2} \quad (21)$$
$$\left(\beta = \frac{f_c}{f_s}\right)$$

The above approximation is correct whenever A is many times greater than σ_N (i.e. high SNR values). For smaller SNR values the simulation can be used to find the error bounds. The comparison between the simulation and that of (21) is represented in Figure 6.

Referring to (21), the value of error depends on both SNR and the value of β. While the value of SNR is not in our hand, it is possible to change the value of β using a suitable sampling frequency. Our simulations show that (as an empirical result) a sampling frequency between 4 and 8 times of f_c results in a good error performance and higher sampling rates do not usually reduce the error considerably. Since the value of f_c is unknown at first, an iterative loop using different sampling frequencies can be used to achieve the best estimate for f_c.

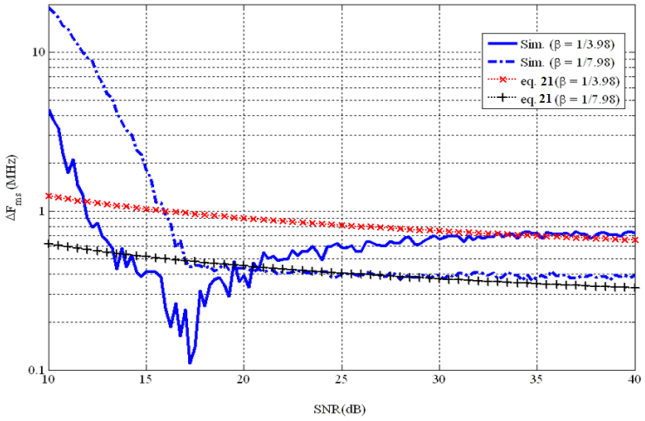

Fig. 6. Comparison between simulated and analytic effect of additive noise

As displayed in Figure 6, for SNR values below 15dB, the approximations made in driving the equations could not be applied. Moreover, it seems that the true value of the rms error is approximately two times greater than what is suggested by the equation. This difference should be analyzed in a further research.

3- 2- Effect of clock jitter

Clock jitter caused by phase noise of the clock oscillator results in sampling points different from the ideal ones. If no clock jitter existed, the samples would be taken at points $t_k=kT_s$, but clock jitter shifts the sampling points to $t_k=kT_s+\Delta t_k$. Here Δtk_s are random variables, usually modeled as a Gaussian process with a standard deviation of σ_J. Whenever the sampling rate is sufficiently greater than f_c, none of the clock jitters inside the sampling window has the effect on the number of zero-crossings and estimated f_c as well. The case of higher f_c values will be discussed later. For now, we will assume that f_s is sufficiently (at least 4 times) greater than f_c. In this case, just if the clock jitters at the first and last samples cause the addition or subtraction of a sample to N_1, then the result will be an error in frequency measurement. It is straightforward to show that the probability of one sample being added to N_1 as a result of clock jitter at the first sample is equal to:

$$P_e = \frac{1}{T_s}\int_0^{T_s} Q\left(\frac{\tau}{\sigma_J}\right)d\tau = \frac{\sigma_J}{T_s}\int_0^{\frac{T_s}{\sigma_J}} Q(x)dx \quad (22)$$

When $\sigma_J \ll T_s$, which is usually the case, the above equation can be simplified as:

$$P_e \cong \frac{\sigma_J}{T_s}\int_0^{+\infty} Q(x)dx = \frac{0.399\sigma_J}{T_s} \quad (23)$$

The effect of one unit error in N_1 value on the estimated frequency, can be calculated by taking the derivative of $\hat{f}_c$ with respect to N_1. Regarding that $N_1 \gg 1$, we have:

$$\frac{d\hat{f}_c}{dN1} \cong \frac{(z-1)f_s}{2}\times -\frac{N_1+1}{(N_1-1)^3} \cong -\frac{(z-1)N_1 f_s}{2(N_1-1)2N_1} = -\frac{f_c}{N_1} \quad (24)$$

Now, with this probability, the mean and rms of frequency measurement error caused by clock jitter are equal to:

$$\mu_f = (1-2P_e-P_e^2)\times 0 + 2P_e \times -\frac{f_c}{N_1} + P_e^2 \times -\frac{2f_c}{N_1} \cong -\frac{2P_e f_c}{N_1}$$
$$\Delta f_{rms} = \sqrt{2P_e\times\left(-\frac{f_c}{N_1}\right)^2 + P_e^2\times\left(-\frac{2f_c}{N_1}\right)^2} \cong \frac{\sqrt{2P_e}f_c}{N_1} \quad (25)$$

In the above equation, it is noticed that P_e is very smaller than 1. Your comment is ok the above equations μf is always much smaller than the quantization error (i.e. N_1 is always a digit) therefore only the rms error may be considerable. This rms error can further be simplified as:

$$\Delta f_{rms} \cong \frac{\sqrt{0.798\sigma_J f_s f_c}}{N_1} \quad (26)$$

Figure 7 compares the result of simulation and the one calculated in (26). Referring to this figure if the input frequency is not in the vicinity of $f_s/2$, then (26) estimates the effect of clock jitter suitably.

3- 3- Effect of comparator bias

Ideally, the sinusoid samples are compared to zero in order to be turned into bits which are used for frequency estimation. In reality, the comparator has a bias voltage equal to b and the samples are compared to this value. It is logical to assume that b is so less than signal amplitude (A); otherwise, the system performance will be awkward. Given this assunmption, the k^{th} zero-crossing (threshold-crossing) point is shifted by Δt_k seconds according to the following equation:

$$A\sin\left(2\pi f_c\left(\frac{kT_c}{2}+\Delta t_k\right)\right)=b$$

$$\Rightarrow A\sin\left(k\pi f_c T_c\right)+2A\pi f_c\cos\left(k\pi f_c T_c\right)\Delta t_k\cong b \qquad (27)$$

$$\Rightarrow \Delta t_k=\frac{(-1)^k b}{2A\pi f_c}=(-1)^k\Delta t \qquad \left(\Delta t=\frac{b}{A\omega_c}\right)$$

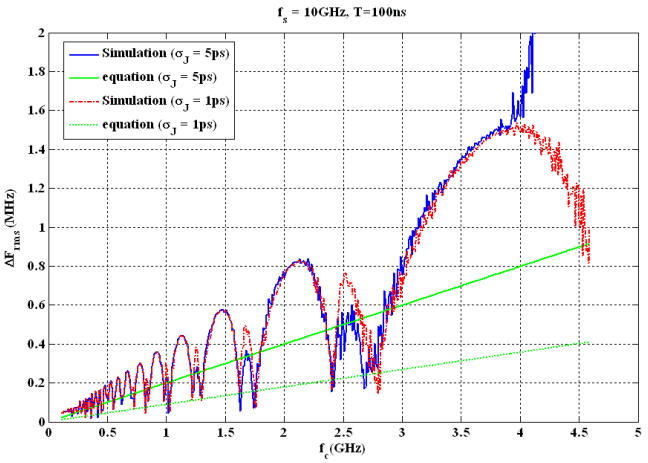

Fig. 7. The effect of clock jitter (a comparison between equation 28 and simulation).

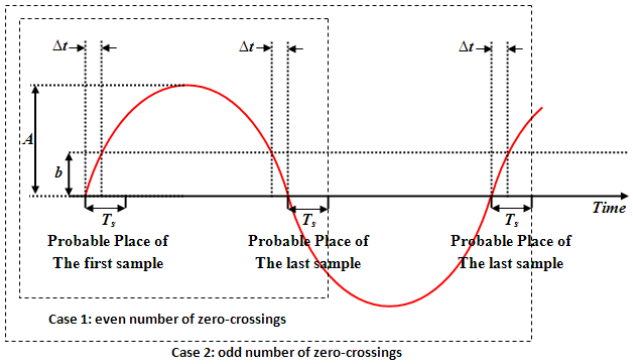

Fig. 8. Different effects of bias voltage on zero-crossing points

This change that occurrs inside the sampling window cannot change the number of zero-crossings. But at the first and last samples, it can change the total number of samples, (N_1) hence, changing the estimated frequency. The effect of this error is different when the number of zero-crossings is even or odd, also the result is different when is smaller or greater than one sampling period (T_s). These different situations are shown in Figure 8. According to this figure, for both cases, namely 1 and 2, when $\Delta t<T_s$, the probability of one sample error at the beginning and at the end is equal to $P=\Delta t/T_s$. Hence, the rms frequency error due to unwanted bias is equal to the follwoing:

$$\Delta f_{rms}=\sqrt{2P}\Delta F=\sqrt{\frac{bf_s}{\pi A f_c}}\frac{f_c}{N_1}=\frac{1}{N_1}\sqrt{\frac{bf_s f_c}{\pi A}} \qquad (28)$$

When $\Delta t>T_s$, for case 1, the following error occurs due to bias voltage:

$$\Delta f\cong\frac{2\Delta t}{T_s}\frac{f_c}{N_1}=\frac{b}{\pi A}\frac{f_s}{N_1} \qquad (29)$$

This value is a possible error due to comparator bias. For case 2, the errors at the beginning and the end, compensate each other, and at most one unit change is introduced to N_1 value. Thus, the error, in this case, is equal to:

$$\Delta f\cong\frac{f_s}{N_1} \qquad (30)$$

4- Overview of proposed scheme

In the previous sections, the optimal frequency estimation algorithm in mono-bit IFM was described and different factors affecting the performance of the system was analyzed. Here again, we review all the above-mentioned topics in a unified structure, in order to have a better understanding of the proposed system and its performance.

First of all, the sampling frequency (f_s) and the length of sampling window (T) should be determined. Ideally, the sampling frequency should be a little greater than the double of the maximum input frequency. In practice, maximum input frequency may be as high as 40GHz; thus, f_s should be 80GHz or higher. However, with the current technology, such a sampling speed is impossible. Therefore, f_s is determined by affordable technology, then the input signal is divided into sub-bands and is down-converted to frequency bands suitable to be sampled with fs rate. Regarding the recent technology, a sampling rate up to 10GHz is almost possible. With this rate, the collected data can also be analyzed in a real time.

The sampling period, sat T, is determined regarding quantization error. The highest input frequency is almost $f_s/2$. Refer to Table 1. For this frequency, the quantization error is equal to $0.16f_s/N_1$ which is around 0.16/T. Hence, if a frequency error up to ΔFmax is acceptable, then the sampling period should be selected equal to or greater than 0.16/ΔFmax.

After signal sampling, the processing algorithm should be performed. This algorithm is represented in Figure 9. In this figure, if the comparator bias is ignorable, then the section devoted to this part can be omitted. Also, if the system is not to work in a busy environment, then the part devoted to "Pulse-on-Pulse" processing could also be omitted, reducing the computational load considerably.

The causes of error in the system are listed in Table 1. The quantization error was discussed earlier. The other errors should be about quantization error or less. For thermal noise according to Figure 12, at an SNR equal to or higher than 15dB, in the worst case, the error is about 0.25/T, less than two times that of the quantization error. Therefore, it seems that a 15dB SNR is almost suitable in order to have an acceptable performance; however, a 20dB SNR is recommended for a guaranteed performance.

Referring to Table 1, the worst clock jitter effect occurs at highest input frequency ($f_s/2$). For this input frequency, the error due to clock jitter is almost equal to $\sqrt{0.2\sigma_J f_s}/T$. This value should be less than or equal to 0.16/T. Thus we should have $\sigma_j<0.128\ f_s$.

The worst comparator bias effect occurs at highest input frequency ($f_s/2$). At this input frequency, the error is equal to $\sqrt{b/2\pi A}/T$ Hence, $\sqrt{b/2\pi A}$ should be less than 0.16. This results in the inequality $b<0.16A_{min}$. The results of this section are given in Table 2.

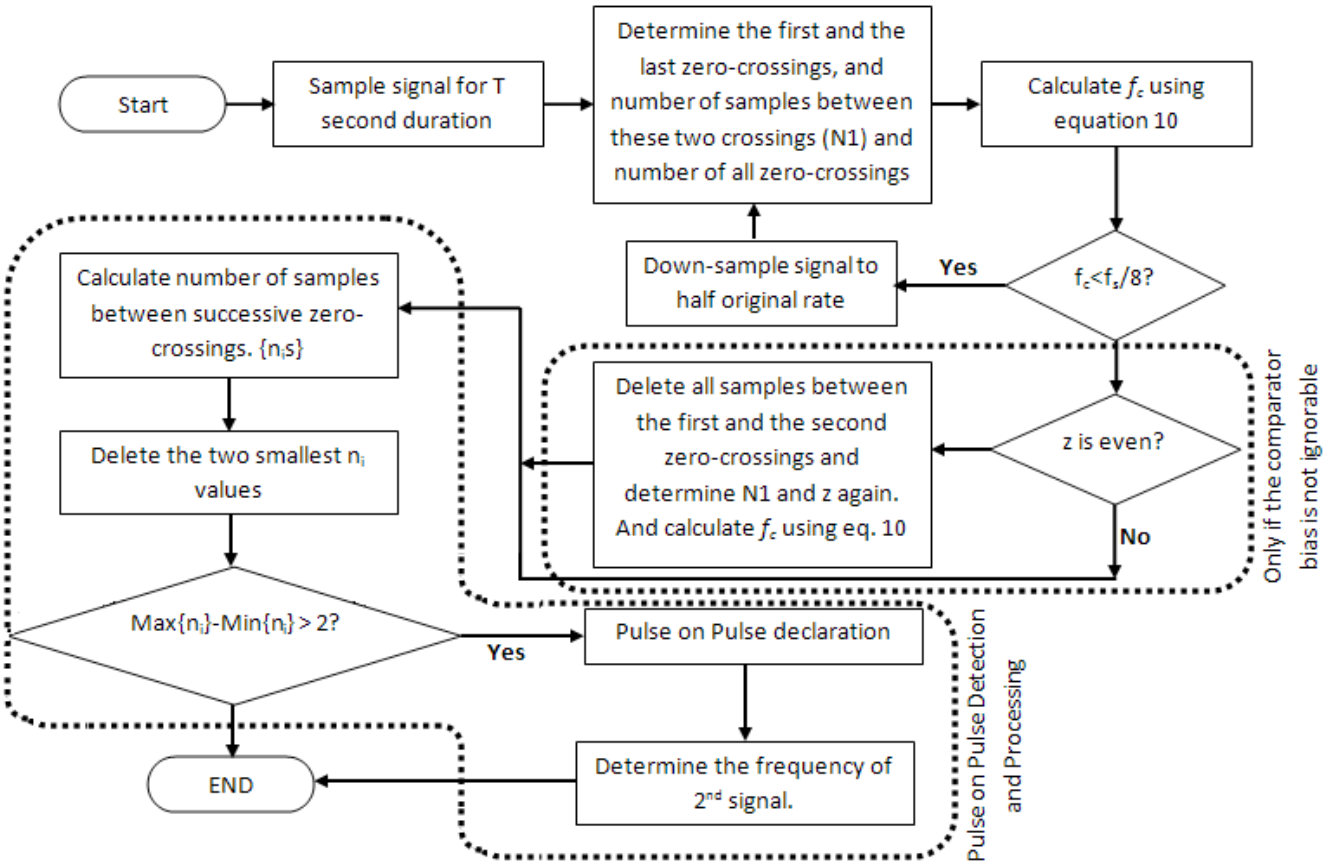

Fig. 9. The algorithm of zero-crossing mono-bit IFM

Table 1. Different sources of error in mono-bit DIFM

Error Type	Value	Note
Quantization (Finite Sampling Rate)	$\frac{0.32 f_s}{N_1}$	
Thermal (Additive)	$\frac{f_s}{N_1}\sqrt{\frac{Q\left(\gamma\sin\left(2\pi\beta\right)\right)}{7.88}+\frac{\gamma^{-0.92}\beta^2}{1.96}}$	$\beta=\frac{f_c}{f_s},\gamma=\frac{A}{\sigma_N}$
Clock Jitter	$\frac{f_c}{N_1}\sqrt{0.798\sigma_J f_s}$	
Comparator Bias	$\frac{1}{N_1}\sqrt{\frac{b f_s f_c}{\pi A}}$	b is system bias
Pulse on Pulse	No Considerable effect on stronger signal if ΔP is greater than 6dB	Can be detected by variation in the distance of consequent zero-crossings

Table 2. System design consideration

No.	Cause of error	Acceptable Value	Note
1	Sampling rate	$f_s = 2f_{Max}$	Or most affordable frequency
2	Sampling period	$T > \frac{0.16}{\Delta F_{Max}}$	
3	SNR	>15dB	>20dB is recommended
4	Clock Jitter	$\sigma_J < \frac{0.128}{f_s}$	
5	Comparator bias	$b < 0.16\ A_{Min}$	

5- CONCLUSION

In this paper, the performance of mono-bit digital IFM device was analyzed. It was shown that how the performance of the original system can be modified using a minor change in the algorithm. Then, different causes of error in this system were analyzed, and some closed form approximate equations describing each error were derived. The effect of the pulse-on-pulse occurrence and the effect of input frequencies near the Nyquist rate were discussed. Finally, we presented a flowchart describing the whole algorithm for the system as well as the considerations necessary for the system design.

REFERENCES

[1] H. Gruchala, M. CzyzEwski, The instantaneous frequency measurement receiver in the complex electromagnetic environment, in: Microwaves, Radar and Wireless Communications, 2004. MIKON-2004. 15th International Conference on, IEEE, 2004, pp. 155-158.

[2] R.G. Wiley, ELINT: The interception and analysis of radar signals, Artech House, 2006.

[3] A.B. Carlson, Communication system, Tata McGraw-Hill Education, 2010.

[4] A. Weiss, B. Friedlander, Simultaneous signals in IFM receivers, IEE Proceedings-Radar, Sonar and Navigation, 144(4) (1997) 181-185.

[5] P. East, Design techniques and performance of digital IFM, in: IEE Proceedings F (Communications, Radar and Signal Processing), IET, 1982, pp. 154-163.

[6] J. Hedge, W. McCormick, J.B. Tsui, IFM receiver with two correlators, in: Aerospace and Electronics Conference, 1989. NAECON 1989., Proceedings of the IEEE 1989 National, IEEE, 1989, pp. 898-901.

[7] H. Gruchala, M. CzyzEwski, The instantaneous frequency measurement receiver in the complex electromagnetic environment, in: Microwaves, Radar and Wireless Communications, 2004. MIKON-2004. 15th International Conference on, IEEE, 2004, pp. 155-158.

[8] H. Gruchalla, M. Czyzewski, A. Slowik, The Instantaneous Frequency Measurement Receiver with Simultaneous Signal Capability, in: Microwaves, Radar & Wireless Communications, 2006. MIKon 2006. International Conference on, IEEE, 2006, pp. 554-557.

[9] M. Thornton, Ultra-broadband frequency discriminator designs for IFM receivers, in: Multi-Octave Active and Passive Components and Antennas, IEE Colloquium on, IET, 1989, pp. 13/11-13/14.

[10] S.C. Sekhar, T.V. Sreenivas, Adaptive window zero-crossing-based instantaneous frequency estimation, EURASIP Journal on Advances in Signal Processing, 2004(12) (2004) 249858.

[11] X. Zou, H. Chi, J. Yao, Microwave frequency measurement based on optical power monitoring using a complementary optical filter pair, IEEE Transactions on Microwave Theory and Techniques, 57(2) (2009) 505-511.

[12] X. Zou, J. Yao, An optical approach to microwave frequency measurement with adjustable measurement range and resolution, IEEE photonics technology letters, 20(23) (2008) 1989-1991.

[13] J. Helton, C.-I.H. Chen, D.M. Lin, J.B. Tsui, FPGA-based 1.2 GHz bandwidth digital instantaneous frequency measurement receiver, in: Quality Electronic Design, 2008. ISQED 2008. 9th International Symposium on, IEEE, 2008, pp. 568-571.

[14] J.B. Tsui, Digital techniques for wideband receivers, SciTech Publishing, 2004.

[15] P. Gibson, A 9 Bit DIFM Receiver for Ka-Band, in: Microwave Conference, 1985. 15th European, IEEE, 1985, pp. 599-604.

[16] http://www.mw-elisra.com/pdf/DIFM%202-18.pdf

[17] http://www.inphi- corp.com/docs/Inphi_Military_and_Aerospace_Solutions_Guide.pdf

[18] A.A. Ivanov, O.G. Morozov, V.A. Andreev, A.A. Kuznetsov, L.M. Faskhutdinov, Radiophotonic method for instantaneous frequency measurement based on principles of "frequency-amplitude" conversion in Fiber Bragg grating and additional frequency separation, in: Antenna Theory and Techniques (ICATT), 2017 XI International Conference on, IEEE, 2017, pp. 425-428.

[19] M. Burla, X. Wang, M. Li, L. Chrostowski, J. Azaña, On-chip instantaneous microwave frequency measurement system based on a waveguide Bragg grating on silicon, in: CLEO: Science and Innovations, Optical Society of America, 2015, pp. STh4F. 7.

[20] B. De Oliveira, M. de Melo, I. Llamas-Garro, M. Espinosa-Espinosa, M.T. de Oliveira, E. de Oliveira, Integrated instantaneous frequency measurement subsystem based on multi-band-stop filters, in: Microwave Conference (APMC), 2014 Asia-Pacific, IEEE, 2014, pp. 910-912.

[21] F. Marvasti, Nonuniform sampling: theory and practice, Springer Science & Business Media, 2012.

[22] P. Stoica, R.L. Moses, Introduction to spectral analysis, Prentice hall Upper Saddle River, NJ, 1997.

[23] W.A. Gardner, Statistical Spectral Analysis: A Nonprobabilistic Approach, in, Prentice Hall, Englewood Cliffs, NJ, 1988.

Please cite this article using:

Y. Norouzi, H. Shahbazi, S. Mirzaei, Performance Analysis Of Mono-bit Digital Instantaneous Frequency Measurement (Difm) Device, *AUT J. Elec. Eng.,* 49(2)(2017)131-140.

DOI: 10.22060/eej.2017.12155.5050